

# First Surface Measurement of Cloud Condensation Nuclei over Kanpur, IGP: Role of Long Range Transport

V. Patidar, S. N. Tripathi, P. K. Bharti, and Tarun Gupta

Department of Civil Engineering, Indian Institute of Technology, Kanpur, India

Measurements have been carried out for cloud condensation nuclei ( $N_{CCN}$ , number concentration at 0.38% average depleted supersaturation, SS) and submicron aerosol ( $N_{CN}$ ), using a CCN (cloud condensation nuclei) counter (Droplet Measurement Technology) and Scanning Mobility Particle Sizer (TSI), respectively, for a large number of days in each season of the year 2008 and 2009 at Kanpur, North India. Aerosol chemical composition was also measured for 3 days and 3 nights during November–December 2009.  $N_{CCN}$  was generally much higher than observed at similar environments elsewhere except in Chinese cities. Due to higher loading of CCN the supersaturation depletion correction is applied. Significant intraseasonal variability was observed in  $N_{CCN}$  and CCN/CN ratio ( $N_{CCN}/N_{CN}$ ), due to different air masses coming from north–west, east, and central parts of India. The CCN concentrations at 0.38% and CCN/CN ratio for the year 2008 varied between 10,043–12,107  $\text{cm}^{-3}$  and 0.12–0.30 in winter season and 5942–7184  $\text{cm}^{-3}$  and 0.07–0.15 in premonsoon season, respectively. For 2009, it varied between 10,518–13,029  $\text{cm}^{-3}$  and 0.28–0.53 in winter season and 3596–8040  $\text{cm}^{-3}$  and 0.20–0.28 in postmonsoon season, respectively. Higher CCN/CN ratio was observed during winter season when the air mass came from north–west, central, and eastern landmass of India. This was most likely due to relatively high accumulation mode particle concentration and large number of forest fires observed in those regions. As expected, polluted continental air masses lead to a significant increase in CCN concentrations over the winter months, most likely due to increased anthropogenic activities, i.e., increased fuel usage, large biomass burning coupled with lower mixed boundary layers. A closure study was performed by application of Köhler theory, utilizing chemical composition, and size distribution measured by SMPS. CCN concentrations were predicted for 3 days and 3 nights and these values were compared with measured CCN values at 0.13, 0.33, and 0.64% SS. In the present closure study, CCN values were slightly overpredicted to the extent of  $21\% \pm 18\%$ .

[Supplementary materials are available for this article. Go to the publisher's online edition of *Aerosol Science and Technology* to view the free supplementary files.]

## 1. INTRODUCTION

The concentration of cloud condensation nuclei (CCN) can significantly affect cloud microphysical processes, and in turn, several aspects of weather and climate. The aerosol–cloud interactions and its impact on climate is the least understood and therefore is a subject of intense research in recent years. For more details pertaining to the effects of aerosols on climate and on cloud processes and precipitation, one can look into the excellent reviews by (Lohmann and Feichter 2005; Rosenfeld et al. 2008).

Aerosols, by acting as CCN, can perturb clouds. Their effect on earth radiative balance is the largest source of uncertainty in anthropogenic climate change (Houghton et al. 2001). A strong positive correlation exists between cloud droplet number concentration and CCN concentration, implying an increase in CCN number results in increased droplet concentration that increases reflectivity leading to climate cooling (Ramanathan et al. 2001).

This has been confirmed by both modeling results and field observations in marine and continental environments (Ramanathan et al. 2001). Therefore, simultaneous *in-situ* measurements of cloud condensation nuclei and aerosol properties are crucial for establishing a quantitative relationship between cloud microphysics and the microphysical (size) and chemical properties of aerosol (Rissman et al. 2006). Amongst several outstanding issues, the most important is the creation of seasonal 3-D maps of the global distribution of CCN, which is most relevant to warm cloud formation. Considerable efforts have been made in recent years to construct a global CCN climatology, e.g., Southern Ocean (Hudson et al. 1998; Yum and Hudson 2004), northeast Pacific and Atlantic Ocean (Hudson and Xie 1999), Arctic Ocean (Yum and Hudson 2001), China Ocean (Lixin and Ying 2007), Korea Ocean (Kuwata et al. 2007), Indian Ocean (Hudson and Yum 2002), and relatively polluted locations where anthropogenic emissions contribute significantly to surface CCN (Hudson et al. 1991).

Received 28 December 2010; accepted 7 March 2012.

This study was carried out with support from Department of Science and Technology, Continental Tropical Convergence Programme and ISRO GBP programme. We acknowledge the help of Monika Srivastava, Anubhav Kumar Dwivedi, and Rosalin Dalai in revising the manuscript.

Address correspondence to S. N. Tripathi, Department of Civil Engineering, Indian Institute of Technology Kanpur, Kanpur 208016, India. E-mail: snt@iitk.ac.in

Lixin and Ying (2007) performed ground based and aircraft measurements of CCN in Shijiazhuang city at 0.1%, 0.3%, and 0.5% SS (supersaturation) during June–August 2005. Ground measurements of CCN data show a large difference in concentration at the same SS (Snider et al. 2003). The minimum and maximum concentrations at 0.5% SS were  $2431 \text{ cm}^{-3}$  and  $21812 \text{ cm}^{-3}$ , respectively. Kuwata et al. (2007) measured CCN concentration and the size distributions of CCN/CN ratios at SS of 0.097%, 0.27%, 0.58%, and 0.97% at Jeju Island, Korea in March–April 2005. The CCN concentration at 0.97% SS was measured to be  $5292 \pm 1551 \text{ cm}^{-3}$ . The CCN concentrations were found to be higher compared to other remote areas of the world such as Island of Tasmania in Australia and Mace Head in Ireland due to transported anthropogenic aerosol. Yum and Hudson (2005) performed CCN measurements with the CCN spectrometer at the Korea Global Atmosphere Watch (GAW) Observatory (KGAWO) on the west coast of Korean peninsula. Data was classified as maritime or continental according to the air mass back trajectories. The average continental CCN concentration at 1% SS was  $5292 \pm 1551 \text{ cm}^{-3}$ .

Each particle requires a discrete amount of water vapor to activate into a cloud droplet. Köhler theory describes the critical SS above which particle of a given size and composition can freely grow into a cloud droplet by condensation. Recently, several researchers have proposed modifications to Köhler theory to include additional effects that organic compounds, soluble, or insoluble, have on surface tension of droplet solution. Cloud droplet formation is based on the thermodynamic equilibrium conditions and depends on the equilibrium saturation ratio of a wet particle of diameter and on the contributions of curvature (Kelvin) and solute (Raoult) terms (Köhler 1936; Seinfeld and Pandis 1998).

CCN closure is the best test of Köhler theory where measured CCN values are compared with predictions made using chemical composition and size distribution measurements. The closure study is successful when the modeled and measured CCN are comparable within measurement uncertainty. CCN closure study has been performed for many years with varying success rates. A summary is given in the Table S1 in the online supplementary material.

Current work presented here provides the CCN and CN data set from a location, which is representative of a highly polluted continental environment (Gupta 2008). In India, efforts have been made to study aerosol microphysical and optical properties in various environments (Singh et al. 2004; Dey and Tripathi 2007), but no study has been carried out to date, to understand CCN behavior and closure study. In this study, the seasonal variation of CCN concentrations over Kanpur covering all major seasons is presented. In addition, the role of long-range transport in influencing surface CCN behavior is explored. Seasonal aerosol distributions for the dominant transport pathways are also presented for the measurement period spanning over the two years 2008 and 2009. Finally, CCN closure study has been performed using

3 day-time and 3 night-time aerosol chemical composition data.

## 2. SITE LOCATION, MEASUREMENT, AND INSTRUMENTATION

### 2.1. Measurement Site

Measurement of polydisperse CCN concentrations and submicron aerosol size distributions and total particle (i.e., condensation nuclei, CN) concentrations were made from 26 January–15 November 2008 and from 27 March–17 December 2009 at Indian Institute of Technology (IIT) Kanpur (longitude  $80^{\circ}13'E$  and latitude  $26^{\circ}30'N$ ), 142 m ASL, i.e., for year 2008, 25, 34, 15, and 49 days of CCN data and, 24, 23, 8, and 30 days of CN was available for winter, premonsoon, monsoon, and postmonsoon seasons, respectively. Whereas for 2009, 14, 17, 17, and 63 days of CCN data and, 13, 10, 7, and 34 days of CN data was available for winter, premonsoon, monsoon, and postmonsoon seasons, respectively. Both the instruments (CCN and SMPS) were collocated during the sampling period. The IIT Kanpur campus is 17 km upwind of the center of Kanpur City. Kanpur is about 1400 km from both the coasts of Bay of Bengal and Arabian Sea. Kanpur is a representative site of the Indo Gangetic Plains (IGP), where anthropogenic and natural aerosols show distinct seasonal characteristics and mixing (Dey et al. 2008). In terms of weather and seasonal variability, Kanpur experiences four seasons: winter (December–February), premonsoon (March–May), monsoon (June–August), and postmonsoon (September–November) (Singh et al. 2004; Tripathi et al. 2005). For entire observation period of year 2008 and 2009, wind was light and variable mostly North–Westerly as shown in Figure S1 in the online supplementary material. In the year 2008, from December–February, the wind speed remains very low in the IGP and mostly calm conditions prevail. The regional wind is mainly northerly to northwesterly. From March onwards, wind became westerly and speed starts increasing, which raises dusts from the soil within the basin and from the arid regions located in the westernmost part of India and Pakistan (the Great Thar Desert) and the Gulf region in the Middle East. During the monsoon season, winds start entering the IGP from southwest and southeast. From October, the wind direction starts changing and become northerly to northwesterly in the winter season. For 2009, the wind direction follows the similar pattern with comparatively more calm conditions as compared to 2008. The monthly averaged surface temperature and relative humidity for both the years 2008 and 2009 over the measurement site are shown in Figure S2 in the online supplementary material.

### 2.2. Instrumentation and Observations

CCN number concentrations ( $\text{cm}^{-3}$ ) were measured using a continuous flow stream wise thermal gradient CCN counter (Droplet Measurement Technologies [DMT]) at three interspersed SS, namely 0.2, 0.5, and 1.0%. Operation of the CCN

counter is described in detail elsewhere (Roberts and Nenes 2005; Lance et al. 2006). The CCN counter was housed in the Fog Chamber Lab of IIT Kanpur at a height of 5 m from the ground level. The sampling probe was nearly 0.5 m in length and had a goose-neck shaped inlet to prevent entry of rain droplets and large particles. The instrument was brand new and calibrated by the manufacturer before commissioning.

Calibration of the CCNC has also been carried out at IIT Kanpur laboratory with  $(\text{NH}_4)_2\text{SO}_4$  and NaCl aerosol to characterize the instrument SS that was found to be in good agreement with manufacturer's calibration curves. The aerosol was generated by an atomizer (TSI model 3079) using  $(\text{NH}_4)_2\text{SO}_4$  ( $0.3 \text{ g l}^{-1}$ ) and NaCl ( $0.1 \text{ g l}^{-1}$ ) aqueous solutions and passed through a denuder for drying it. The dry aerosol was passed through the differential mobility analyzer (DMA) with sheath flow of  $3 \text{ L min}^{-1}$  to generate monodisperse particles. The sheath flow and the sample flow ( $0.3 \text{ L min}^{-1}$ ) were maintained with the help of the HEPA filter. The monodisperse aerosol flow was split in two parts, one to the CPC and other to the CCNC, where at a particular temperature gradient ( $\Delta T$ ), concentration of total particles, ( $N_{\text{CN}}$ ), and concentration of CCN ( $N_{\text{CCN}}$ ) were measured and activation fraction  $N_{\text{CCN}}/N_{\text{CN}}$  was computed. This process was repeated over many classified size particles until  $N_{\text{CCN}}/N_{\text{CN}}$  attained unity. The resulting  $N_{\text{CCN}}/N_{\text{CN}}$  curve (activation) exhibited a sigmoidal shape (see Figure S3 in the online supplementary material). The diameter, at which 50% of the monodisperse particles were activated, i.e.,  $D_{50}$ , was the critical dry particle diameter for CCN activation. It represented the diameter required for the particles with the given composition to be activated as CCN for a given supersaturation (Rose et al. 2008). Kohler theory (Equation (2), Section 3.6) was used to compute critical supersaturation  $S_c$  from  $D_{50}$ , assuming the density and molar mass of  $(\text{NH}_4)_2\text{SO}_4$  as  $1760 \text{ kg m}^{-3}$  and  $0.1321 \text{ kg mol}^{-1}$ , respectively.

Error in the CCN measurements may occur due to instrument malfunctioning, temperature destabilization, fogged condition in Optical Particle Counter, increase in the first stage monitor voltage above 0.2–0.3 Volts, variation in sheath to aerosol flow ratio (ideally it should be 10), etc. (DMT 2004). Measurements for all such cases were excluded in the subsequent analysis. Also, during the transient in the supersaturation, a 60 s waiting time was allowed for the instrument to adjust to the new particle concentration (Rose et al. 2008). DMT's test results conducted on ammonium sulfate show some error in CCN count due to vapor loss and negligible error due to coincidence error. All supersaturations had at least 6000 #/cc maximum count rate. For SS below 0.2%, tests showed a maximum error of 50% in count rate up to maximum concentration tested, i.e.,  $30,000 \text{ cm}^{-3}$  (DMT Manual 2004). At SS higher than 0.3% there were minimal losses (10%). During the sampling period for most of the time CCN concentration was found to be greater than  $5000 \text{ cm}^{-3}$ , which resulted in depletion of supersaturation (Lathem and Nenes 2011). Supersaturation depletion correction has been applied for the entire CCN data presented here following the method of Lathem and Nenes (2011).

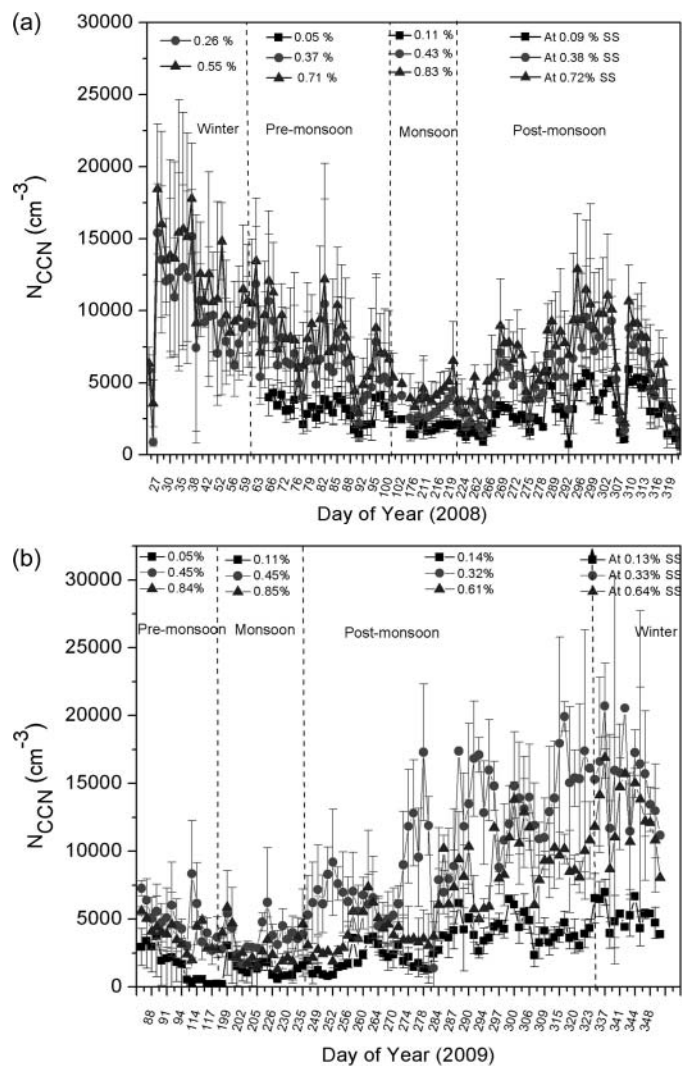


FIG. 1. Time series for 2008 for (a) CCN ( $N_{\text{CCN}}$ ) for four seasonally averaged depleted supersaturations (SS) (b) same as for 2009. Error bar represents the natural variability. The CCN for winter 2008 is not reported as average depleted SS was found to be negative.

Total aerosol number (CN) concentrations and submicron aerosol size distribution were measured by the Scanning Mobility Particle Sizer (TSI Model 3936) with sizes between  $0.014 \mu\text{m}$  and  $0.68 \mu\text{m}$ . Error budget of SMPS has been discussed in detail elsewhere (Baxla et al. 2009; Roy et al. 2009). While operating the instrument the option of coincidence error correction has been selected, thus minimizing the problem of under counting. Multiple charge and diffusional losses corrections were applied using TSI Aerosol Instrument Manager 9.1.0.0.

Time series at seasonally averaged depleted supersaturation corresponding to instrument supersaturation (0.2%, 0.5%, and 1.0% SS) are presented here but results at 0.38% average depleted SS will be discussed in detail. Figures 1a and b show time series of CCN for the complete measurement period during 2008 and 2009 and the corresponding CN time series

is given in the online supplementary material (Figure S4). The CCN and CN concentration was found to be higher during winter and lower during monsoon.

### 2.3. Chemical Composition Measurements

The aerosol chemical composition was determined by analysis of polytetrafluoroethylene (PTFE) filters (Bougiatioti et al. 2009) using PM<sub>1</sub> impaction based aerosol sampler developed in IIT Kanpur (Gupta et al. 2010), where outdoor aerosol was collected for 10 h during day and similarly 10 h during night, by using the method of integrated sampling. In total results of 3 day-time and 3 night-time integrated filter-based PM<sub>1</sub> aerosol samples have been used for closure study. The gravimetric analysis was performed on the filter-collected aerosols to deduce the aerosol concentration. PTFE filters were analyzed for water soluble ions after extraction with milli-Q water with the aid of ultrasonicator. The solutions obtained were analyzed in Ion Chromatograph (Metrohm compact, IC-761) for anions (NO<sub>3</sub><sup>-</sup>, Cl<sup>-</sup>, SO<sub>4</sub><sup>2-</sup>) and cations (Na<sup>+</sup>, NH<sub>4</sub><sup>+</sup>) using detail procedures as described in (Chakraborty and Gupta 2010).

### 2.4. Air Mass Designation

The model vertical velocity, 7 days back trajectory was computed using the Hybrid Single Particle Lagrangian Integrated Trajectory (HYSPPLIT-4) code. Data were analyzed according to back trajectories arriving at noon time (12:00 IST), at the altitude of the observation site. Back trajectory analysis at altitude of the observation site was used in several recent studies for the surface analysis of CCN and aerosols (Rojas et al. 2006). The back trajectories suggest that air mass, originating from both Arabian Sea and Bay of Bengal spent substantial amount of time over land. During winter and premonsoon seasons back trajectories originated only from land areas so they were classified as continental air masses. During monsoon and postmonsoon, significant fractions of back trajectories originated from marine regions that spent substantial time over continental areas, these are referred to as mixed air masses. Accordingly, these data were classified for each season and are shown in Figure S5 in the online supplementary material. It was found that during 2008 in winter and premonsoon, most of the air mass trajectories arrived from North–West continental part of India shown as percentage fractions in parenthesis of Figure S5 and in 2009 same trend was followed for monsoon but in premonsoon percentage fraction was 100% from North–West direction. However, for monsoon and postmonsoon season, entire air mass transport route changed.

## 3. RESULTS AND DISCUSSION

### 3.1. Intraseasonal and Seasonal Variability of CCN Number Concentration

There was considerable inter- and intraseasonal variability in CCN number concentration due to the varying nature of local emissions and the influence of air mass transport routes. For all

the seasons, daily averaged CCN and CN concentrations, for the major transport pathways, were averaged as shown in Table 1. In general, it can be seen that continental CCN are very high throughout all the seasons compared to other reported data for similar environment. Comparing winter and premonsoon seasons, from Table 1, it is evident that CCN concentrations are significantly higher during winter than premonsoon. Hence, for same transport route, a strong seasonal variation in the CCN concentrations was observed. In winter season for both the years  $N_{CCN}$  and  $N_{CN}$  were high due to several reasons, namely, local anthropogenic pollution from fossil fuel burning and increased biomass burning, which gets trapped near the surface due to low boundary layer thickness (Tripathi et al. 2005).

Previous studies (Dey et al. 2004) revealed that in the IGP dust is the major contributor to aerosol loading in the premonsoon and monsoon seasons which possibly contribute little to CCN. Whereas, anthropogenic urban aerosols dominate during the postmonsoon and winter seasons (Mehta et al. 2008), which depending on their chemical composition and size contribute more in terms of CCN in winter season. In premonsoon season, due to high temperature and convection in the atmosphere, the boundary layer expands resulting in a decrease in  $N_{CN}$  within the surface layer due to dispersion of aerosols. In monsoon, rainout and washout are highly effective in removing particulate matter especially the accumulation mode aerosols, which is the main reason for the lowest number concentration.

The seasonal CN concentrations were lower in 2009 and higher in 2008, which can be due to certain factors like in winter, 2009 extent of north–west and central air mass was of short range transport while in 2008 it was long range type transport from both directions. In premonsoon 2009, air mass contribution was basically, from north–west direction but in 2008 contribution was from northwest, eastern, and central direction. During 2008 and 2009, in monsoon and postmonsoon season local anthropogenic pollution can be a significant source for rise in CN concentration. CCN values were also high correspondingly for both these seasons.

Also, considerable intraseasonal variability was seen in CCN and CN number concentration due to the influence of the aerosol transport routes in each season in Figure S5. Overall, continental air masses from eastern part of India are more laden with  $N_{CCN}$  during both winter and premonsoon season (Table 1).  $N_{CCN}$  for eastern route was  $12,107 \pm 3540 \text{ cm}^{-3}$  for winter and  $7184 \pm 2168 \text{ cm}^{-3}$  for premonsoon season. Table 2 also shows average variations of  $N_{CCN}$  and  $N_{CN}$  for monsoon and postmonsoon seasons for mixed and continental air masses. As expected,  $N_{CCN}$  was low for mixed air masses.

CCN/CN (activation fraction) as a function of SS is shown in Figure 2. There is considerable interseasonal variation seen in CCN/CN ratio particularly at high SS. As SS increases CCN/CN generally increases and approaches unity (Bougiatioti et al. 2009), but values of 0.5 or less has also been reported (Rojas et al. 2006) during 2008. However, in 2009, CCN/CN ratio increased for all the three seasons except in premonsoon seasons.

TABLE 1  
Seasonal average surface CCN at various depleted % SS and CN concentration ( $\text{cm}^{-3}$ ) for different transport routes for year 2008 and 2009

Continental air mass				Mixed air mass	CCN/CN aerosol ratio ( $N_{\text{CCN}}/N_{\text{CN}}$ )
<b>Winter (2008)</b>					
$N_{\text{CCN},0.26}$	12,107 ± 3540	10,045 ± 3517	10,043 ± 3249		0.12–0.3
$N_{\text{CN}}$	55,435 ± 17,688	82,693 ± 50,318	37,955 ± 2090		
<b>Winter (2009)</b>					
$N_{\text{CCN},0.13}$	739 ± 1317	5389 ± 1009	5130 ± 1072		0.13–0.29
$N_{\text{CN}}$	42,784 ± 6423	18,601 ± 16,056	24,795 ± 21,010		
$N_{\text{CCN},0.33}$	13,029 ± 2819	12846 ± 2706	10,518 ± 1313		0.28–.53
$N_{\text{CN}}$	46,616 ± 17,978	24,359 ± 24,631	23,124 ± 21,650		
$N_{\text{CCN},0.64}$	16,621 ± 921	15,174 ± 3103	12,869 ± 1757		0.31–0.54
$N_{\text{CN}}$	53,067 ± 25,730	27,813 ± 31991	25,792 ± 28,008		
<b>Premonsoon (2008)</b>					
$N_{\text{CCN},0.05}$	3535 ± 472	3613 ± 982	2531 ± 724		0.03–0.07
$N_{\text{CN}}$	47,871 ± 12,854	75,466 ± 15,031	74,154 ± 39,067		0.07–0.15
$N_{\text{CCN},0.38}$	7184 ± 2168	5942 ± 1956	6341 ± 2895		
$N_{\text{CCN},0.72}$	8235 ± 987	8575 ± 1940	7167 ± 775		0.08–0.17
$N_{\text{CN}}$	47,799 ± 11,128	75566 ± 14180	80,405 ± 44,404		
<b>Premonsoon (2009)</b>					
$N_{\text{CCN},0.06}$		1834 ± 907			0.05
$N_{\text{CN}}$		38,542 ± 29,956			
$N_{\text{CCN},0.45}$		3995 ± 946			
$N_{\text{CN}}$		36,603 ± 22,126			0.11
$N_{\text{CCN},0.84}$		5554 ± 1092			
$N_{\text{CN}}$		36,332 ± 25,932			0.15
<b>Monsoon (2008)</b>					
$N_{\text{CCN},0.11}$	1921 ± 235		1962 ± 168		0.05–0.09
$N_{\text{CN}}$	35,499 ± 7342		21,273 ± 3841		
$N_{\text{CCN},0.43}$	3358 ± 700		2987 ± 470		0.1–0.14
$N_{\text{CN}}$	32,442 ± 3298		21,778 ± 2557		
$N_{\text{CCN},0.83}$	4779 ± 1122		4256 ± 178		0.14–0.19
$N_{\text{CN}}$	33,694 ± 4995		22,342 ± 1197		
<b>Monsoon (2009)</b>					
$N_{\text{CCN},0.11}$	1709 ± 479		1182 ± 288		0.09–0.14
$N_{\text{CN}}$	11,439 ± 7454		8698 ± 5192		
$N_{\text{CCN},0.45}$	2827 ± 1653		2080 ± 337		0.23–0.25
$N_{\text{CN}}$	11,439 ± 7454		8698 ± 5192		
$N_{\text{CCN},0.85}$	4094 ± 1809		3300 ± 624		0.30–0.35
$N_{\text{CN}}$	11,461 ± 7939		10,937 ± 4664		
<b>Postmonsoon (2008)</b>					
$N_{\text{CCN},0.09}$	2861 ± 1364	4441 ± 1110	4196 ± 2302		0.05–0.10
$N_{\text{CN}}$	59,095 ± 14,223	60,174 ± 18,154	40,699 ± 5312		
$N_{\text{CCN},0.38}$	4625 ± 1942	6637 ± 2492	4871 ± 1078		0.08–0.11
$N_{\text{CN}}$	57,102 ± 12,682	59,302 ± 19,993	42,373 ± 9181		
$N_{\text{CCN},0.73}$	6444 ± 1761	9383 ± 2144	7260 ± 1918		0.10–0.17
$N_{\text{CN}}$	59,379 ± 15,424	58,736 ± 17,841	41,853 ± 1105		
<b>Postmonsoon (2009)</b>					
$N_{\text{CCN},0.14}$	2009 ± 674	3830 ± 2070	3720 ± 15,592		0.10–0.12
$N_{\text{CN}}$	19,152 ± 9679	30,619 ± 24,181	30,187 ± 26,434		
$N_{\text{CCN},0.32}$	3596 ± 105	8040 ± 3535	7702 ± 3118		0.20–0.28
$N_{\text{CN}}$	18,174 ± 9037	29,044 ± 24,440	32,021 ± 32,963		
$N_{\text{CCN},0.61}$		9864 ± 4577	10,812 ± 4513		0.37–0.39
$N_{\text{CN}}$		25,121 ± 29,178	28,884 ± 15,495		

TABLE 2  
Seasonal average CN concentrations in Aitken and accumulation modes

Continental air mass, cm <sup>-3</sup> Aitken (0.0146–0.10 μm), Accumulation (0.10–0.685 μm)						
Aerosol mode	Eastern air mass	North-West air mass	Northern air mass	Central air mass	Mixed air mass, cm <sup>-3</sup>	
Winter	Aitken					
	2008	25,512	31,626		18,487	
	2009	14,948	8211		9766	
	Accumulation					
	2008	35,331	32,497		20,507	
	2009	31,088	15,810		17,500	
	Aitken/Accumulation					
	2008	0.722	0.973		0.901	
	2009	0.48	0.51		0.55	
	Modal diameter					
2008	0.126	0.113		0.113		
2009	0.162	0.126		0.151		
Premonsoon	Aitken					
	2008	31,205	38,292		36,918	
	2009		22,289			
	Accumulation					
	2008	21,840	22,772		23,702	
	2009		13,708			
	Aitken/Accumulation					
	2008	1.428	1.680		1.557	
	2009		1.6			
	Modal diameter					
2008	0.101	0.094		0.101		
2009		0.082				
Monsoon	Aitken					
	2008	23,340			15,533	
	2009	10,534			6600	
	Accumulation					
	2008	10,539			7477	
	2009	4508			2397	
	Aitken/Accumulation					
	2008	2.21			2.07	
	2009	2.33			2.75	
	Modal diameter					
2008	0.079			0.076		
2009	0.071			0.055		
Postmonsoon	Aitken					
	2008	30,348		28,452	22,630	
	2009	11,556		13,342	14,556	
	Accumulation					
	2008	25,114		33,564	21,525	
	2009	9700		17,265	16,966	
	Aitken/Accumulation					
	2008	1.20		0.847	1.05	
	2009	1.19		0.77	0.86	
	Modal diameter					
2008	0.105		0.112	0.105		
2009	0.105		0.126	0.126		

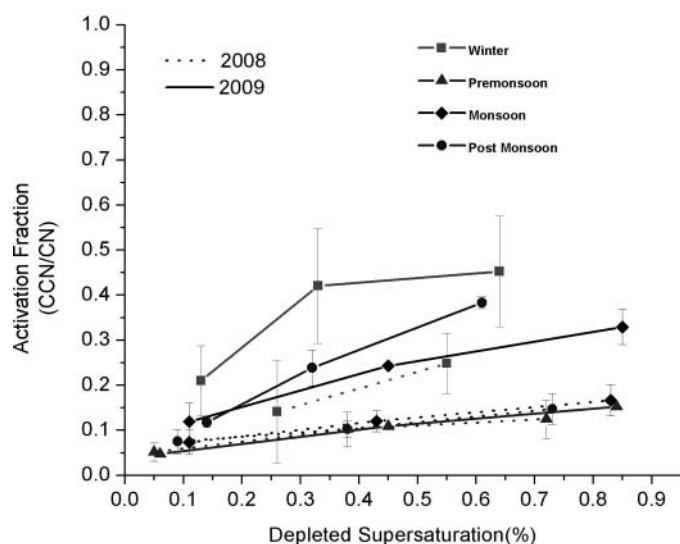


FIG. 2. Activation fraction,  $CCN/CN$ , as a function of  $SS$  for winter, premonsoon, monsoon, and postmonsoon seasons for both the years 2008 and 2009. Error bar represents the natural variability.

Higher  $CCN/CN$  ratio in winter as seen from Table 1 is attributed to relatively higher accumulation mode particle concentration than Aitken as discussed in Section 3.2. Large average  $CCN/CN$  ratio ( $N_{CCN,0.38}/N_{CN}$ ) of 0.26 and 0.45 were observed for both years 2008 and 2009, respectively, when the aerosol was transported from continental India (central part) in winter season. During monsoon  $N_{CCN,0.38}/N_{CN}$  was largest for mixed air mass for 2008 whereas it was largest for continental air mass for 2009 (Table 1).

In year 2008 during postmonsoon season, the average low  $CCN/CN$  ratio was nearly the same irrespective of the air mass transport Northern air mass during postmonsoon has relatively high-accumulation mode particle concentration but the  $CCN/CN$  ratio was only 0.11 during 2008, possibly due to the lack of any fire counts observed, while the ratio increased to 0.28 in the year 2009. The  $CCN/CN$  ratio reported here are rather low compared with the previous studies for continental environments, e.g., over the Puy de Dôme, France (Rojas et al. 2006) where  $CCN/CN$  ratio was 0.3–0.4. The  $CCN/CN$  ratio over Durham, New Hampshire, reconstructed using the values from Table 1 and Equation 1 of (Medina et al. 2007), was approximately equal to 0.68–0.75 at 1%  $SS$ , which is quite high compared with the present study.

MODIS Hotspots/Active fire counts over India, in winter season, showed that forest fire was more concentrated in central part of India, while in premonsoon most of the fire counts were found in the eastern region of India. Northeast India and Bengal/Orissa were characterized by large and frequent ATSR (Along-Track Scanning Radiometer) fire count signals as shown in past studies (Duncan et al. 2003). Thus, the observed variability in  $CCN/CN$  ratio may be due to several processes,

which include local pollution sources, origin of the air mass, and hygroscopicity of the aerosols.

### 3.2. Submicron Aerosol Size Distribution

Average aerosol size distributions (0.014–0.68  $\mu\text{m}$ ) measured using SMPS are presented for each season in Figure S6 as given in the online supplementary material, (Baxla et al. 2009). Seasonal changes in the aerosols size distributions for each year can be easily observed by comparing the relative amplitude of each mode with the maximum concentration during winter and minimum during monsoon season. The average aerosol ( $CN$ ) concentrations during year 2008 were  $56,624 \pm 2508 \text{ cm}^{-3}$  and  $27,838 \pm 657 \text{ cm}^{-3}$  in winter and monsoon, respectively, while in year 2009  $CN$  concentrations were  $31,883 \pm 3444 \text{ cm}^{-3}$  and  $11,203 \pm 1137 \text{ cm}^{-3}$ . There is a persistent accumulation mode throughout both the years 2008 and 2009 where concentration increases from postmonsoon with a steady broadening. The accumulation particles were found with mode between 76 nm and 126 nm for 2008 and 55 nm and 162 nm for 2009, and their concentration as well as their contribution to the total particle number was maximum in winter and minimum in monsoon. The characteristic parameters of the seasonal aerosol size distribution for different air masses are given in Table 2. In monsoon season, rainout and washout are highly effective in aerosol removal especially accumulation mode aerosols, from the atmosphere. A decrease in concentrations of both accumulation mode aerosols and  $CCN$  was found which is in agreement with our  $CCN$  measurements. These results can be compared to the aerosol size distribution seasonal analysis performed by (Venzac et al. 2008) which shows the accumulation particles with a mode between 135 nm and 145 nm over the Puy de Dôme, France.

### 3.3. Diurnal Variability of $CCN$ Number Concentration

Figure 3a and b shows the diurnal variation of  $CCN$  at various depleted supersaturation each season for a period from 26 January to 15 November 2008 and from 26 March to 17 December 2009, respectively. Strong (winter) to mild (monsoon) diurnal trends were observed in the  $CCN$  concentrations measured at Kanpur for both the year 2008 and 2009.  $CCN$  concentrations show maximum departure from the daily mean in the early morning for all the seasons. The diurnal trend follows similar pattern for all the seasons. The strong diurnal cycle of  $CCN$  concentrations may be attributed to the diurnal cycle of local pollutants arising from anthropogenic activities and the planetary boundary layer evolution.

### 3.4. Aerosol Mass and Composition Measurements

The average concentrations of ionic species during the measurement period for  $PM_{10}$  were  $8.69 \pm 6.03 \mu\text{g m}^{-3}$  and  $13.42 \pm 9.56 \mu\text{g m}^{-3}$  for day time and night time, respectively. Mass concentration of Nitrate and Ammonium are comparatively higher than other species. During December, there is increase in concentration of each species which is probably due to fog processing (Tare et al. 2006; Tripathi et al. 2006).

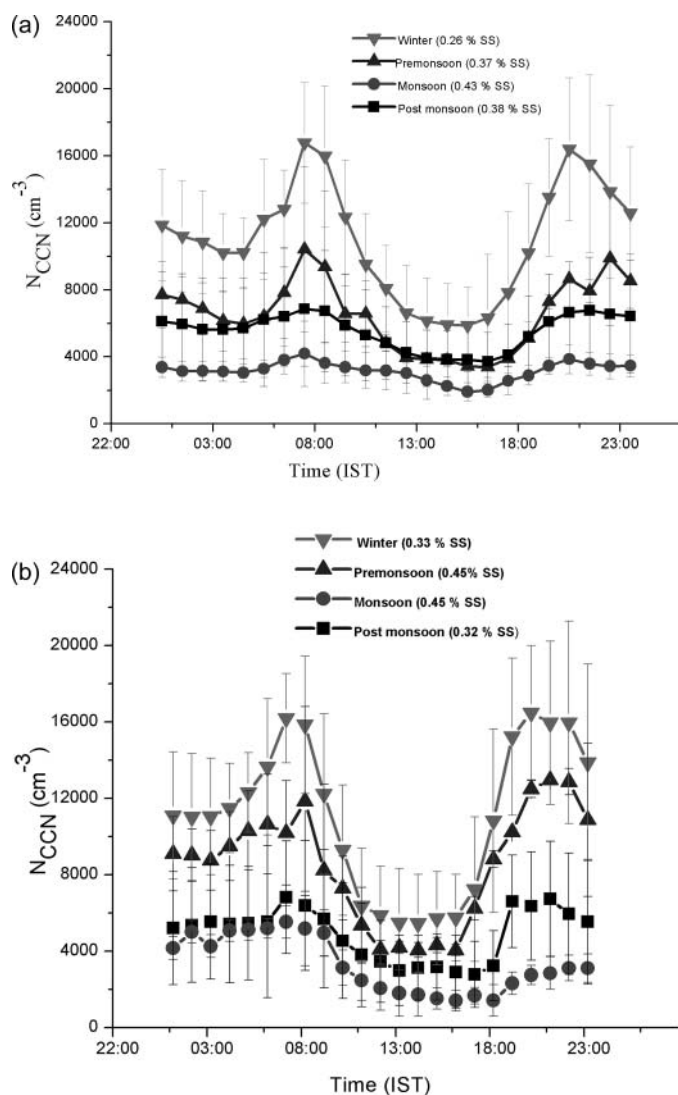


FIG. 3. Diurnal variation of CCN at various seasonally-averaged depleted SS (a) for year 2008 (b) for year 2009. Error bar represents the natural variability.

### 3.5. CCN Closure

A closure study was performed for three days and three nights during November–December, 2009. Each 12-min CCN data for different supersaturation was examined for (1) minimal fluctuations in the flow chamber temperature gradient and (2) stability of the flows. Small fluctuations in temperature have a minimal impact on the supersaturation and closure (Ervens et al. 2007). If both criteria were satisfied then the CCN concentrations were averaged corresponding to each concurrent scan of SMPS for every supersaturation segment. The chemical composition for computing CCN properties was obtained from the analysis of corresponding 10-h PM<sub>1</sub> filtersamples for day-time and night-time, respectively. The species that have been used for the closure analysis are ammonium sulfate and organics. Ammonium and Sulfate ions obtained from the PM<sub>1</sub> filters analysis were synthesized to form ammonium sulfate by

regression analysis of experimental NH<sub>4</sub><sup>+</sup> ion with respect to the ambient NH<sub>4</sub><sup>+</sup> ion in the form of (NH<sub>4</sub>)<sub>2</sub>SO<sub>4</sub> for the complete dataset (Mandaria 2010). While predicting CCN concentrations, it is assumed that aerosol is composed of (NH<sub>4</sub>)<sub>2</sub>SO<sub>4</sub> (which acts as solute) and organics (which do not contribute to the solute, i.e., are hydrophobic) (Medina et al. 2007). The influence of other inorganic species was assumed to be negligible (Medina et al. 2007; Frank et al. 2006; Dusek et al. 2003).

The ability of a particle to act as CCN depends on its chemical composition (volume fraction of solute) and its size. The volume fraction of the solute (ammonium sulfate) was calculated as,

$$\epsilon_s = \frac{\frac{m_s}{\rho_s}}{\frac{m_s}{\rho_s} + \frac{m_i}{\rho_i}} \quad [1]$$

where  $m_s$  and  $m_i$  are the mass of (NH<sub>4</sub>)<sub>2</sub>SO<sub>4</sub> and organics and  $\rho_s$  and  $\rho_i$  are the density of (NH<sub>4</sub>)<sub>2</sub>SO<sub>4</sub> (1760 kg m<sup>-3</sup>) and insoluble organics assuming (1000 kg m<sup>-3</sup>), respectively. For the whole measurement period, ammonium sulfate accounts for approximately  $12.64 \pm 3.70\%$  of the total PM<sub>1</sub> mass and  $\epsilon_s$  has the mean value of  $0.11 \pm 0.04$ . The critical dry particle diameter is calculated by the application of Kohler theory as given in the following equation:

$$S_c = \left[ \frac{256}{27} \left( \frac{M_w \sigma}{RT \rho_w} \right)^3 \left( \frac{M_s}{\rho_s} \right) \left( \frac{\rho_w}{M_w} \right) \frac{D_p^{-3}}{\epsilon_s v_s} \right]^{1/2} \quad [2]$$

Where  $M_w$  (0.01801 kg mol<sup>-1</sup>) and  $M_s$  (0.1321 kg mol<sup>-1</sup>) are the molar mass of water and (NH<sub>4</sub>)<sub>2</sub>SO<sub>4</sub>, respectively,  $R$  is the universal gas constant and  $T$  is the ambient temperature. The effective van't hoff factor  $v_s$  (which includes the effect of osmotic coefficient) is taken as 2.5 (Medina et al. 2007) and  $\sigma$ , the surface tension of water = 0.07197 J m<sup>-2</sup>. Substituting  $\epsilon_s$  in Equation (2) makes it possible to calculate for a given  $S_c$  (in this case, the SS set in the CCN counter), the value of critical dry particle diameter,  $D_p$ . All particles larger than  $D_p$  will activate as CCN. We integrated the size distribution measured by the SMPS from  $D_p$  upto the largest measured size, which gives the predicted CCN concentration (Jurányi et al. 2010; VanReken et al. 2003).

Figure 4 shows the predicted against measured CCN concentrations for 3 days and 3 nights during November–December 2009 assuming that total organic is insoluble. The results show average overprediction of  $21 \pm 18\%$  whereas under prediction of  $5 \pm 30\%$  for 0.13% SS and over prediction of  $11 \pm 32\%$  and  $47 \pm 38\%$  at supersaturation of 0.33% and 0.64%, respectively. The prediction errors would be even larger if a fraction of organics were considered as soluble.

### 3.6. Discussion and Sensitivity Analysis of Closure Study

The present closure study shows on average overprediction that can be attributed to several factors such as due to the overestimation of the sulfate fraction (Bougatioti et al. 2009; Lance et al. 2009), systematic uncertainties in the SMPS



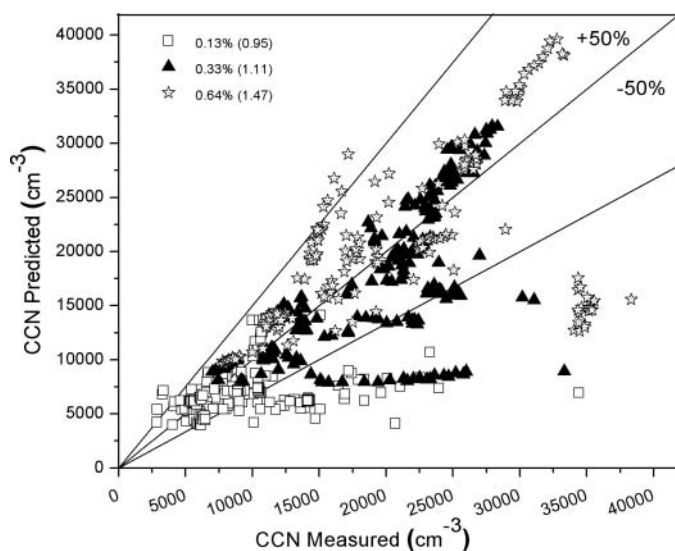


FIG. 4. CCN predicted versus CCN measured at three SS of 0.13%, 0.33%, and 0.64% with corresponding CCN predicted to measured ratio.

and CCN counter measurements (Chang et al. 2007). The overprediction in the present closure study can also be due to lack of size dependent chemical composition and assumption of internal mixing. We found a 10% reduction in solute mass leads to 5% improvement in over prediction at SS of 0.13% and 0.33% while only 3% improvement at SS of 1%.

#### 4. CONCLUSIONS

This paper analyzes the role of long-range transport and different nature of emission on the intra- and interseasonal variation of CCN over a polluted continental site in the Ganga basin. The main conclusions drawn from the study are summarized as follows:

1. Considerable intra seasonal variability of CCN and CCN/CN ratio ( $N_{CCN}/N_{CN}$ ) was found due to differences in the directions of air masses in all the seasons. For both winter and premonsoon seasons, highest CCN concentrations were found for eastern continental transport routes whereas the highest CCN–CN ratio (0.30) was found in winter when the air masses came from central and eastern continental parts of India while in year 2009, the CCN/CN ratio was 0.53 for the similar air mass trend.
2. Strong seasonal variability of CCN was found with highest CCN concentrations in winter and lowest in monsoon season due to cloud and precipitation scavenging.

This dataset will be valuable in developing new (or modification of existing) aerosol-cloud parameterization schemes in Regional Climate Models to assess the regional impacts of changing CCN concentrations on indirect radiative forcing. CCN concentrations were calculated using chemical composition and number size distribution coupled with simple Köhler theory. Predictions were then compared with the measured CCN

concentrations for three different SS 0.13%, 0.33%, and 0.64%, resulting in an overprediction at all the supersaturations except for 0.13%, where it was predicted.

#### REFERENCES

- Baxla, S. P., Roy A. A., Gupta, T., Tripathi S. N., and Bandyopadhyaya R. (2009). Analysis of Diurnal and Seasonal Variation of Submicron Outdoor Aerosol Mass and Size Distribution in a Northern Indian City and its Correlation to Black Carbon. *Aerosol Air Quality Res.*, 9:458–469.
- Bougiatioti, A., Fountoukis, C., Kalivitis, N., Pandis, S. N., Nenes, A., and Milhalopoulos, N. (2009). CCN Closure and Droplet Growth Kinetics. *Atmos. Chem. Phys. Discuss.*, 9:10,303–10,336.
- Chakraborty, A., and Gupta, T. (2010). Chemical Characterization and Source Apportionment of Submicron (PM<sub>1</sub>) Aerosol in Kanpur Region, India. *Aerosol Air Qual. Res.*, 10:433–445.
- Chang, R. Y. W., Liu, P. S. K., Leaitch, W. R., and Abbatt, J. P. D. (2007). Comparison of Measured and Predicted CCN Concentrations at Egbert, Ontario: Focus on the Organic Aerosol Fraction at a Semi Rural Site. *Atmos. Environ.*, 41:8172–8182.
- Dey, S., and Tripathi, S. N. (2007). Estimation of Aerosol Optical Properties in the Ganga Basin, Northern India During the Winter Time. *J. Geophys. Res.*, 112:D03203. DOI: 10.1029/2006JD007267.
- Dey, S., Tripathi, S. N. and Mishra, S. K. (2008). Probable Mixing State of Aerosols in the Indo-Gangetic Basin, Northern India. *Geophys. Res. Lett.*, 35:L03808. DOI: 10.1029/2007GL032622.
- Dey, S., Tripathi, S. N., Singh, R. P., and Holben, B. N. (2004). Influence of Dust Storms on the Aerosol Optical Properties Over the Indo-Gangetic Basin. *J. Geophys. Res.*, 109:D20211. DOI: 10.1029/2004JD004924.
- Droplet Measurement Technologies. (2004). *Cloud Condensation Nuclei Counter Operator Manual S/N: 049, DOC-0086 revised DDMT*.
- Duncan, B. N., Martin, R. V., Staudt, A. C., Yevich, R., and Logan, J. A. (2003). Interannual and Seasonal Variability of Biomass Burning Emissions Constrained by Satellite Observations. *J. Geophys. Res.*, 108(D2):4100. DOI: 10.1029/2002JD002378.
- Dusek, U., Covert, D., Wiedensholer, A., Neuss, C., Weise, D., and Cantrell, W. (2003). Cloud Condensation Nuclei Spectra Derived from Size Distributions and Hygroscopic Properties of the Aerosol in Coastal Southwest Portugal During ACE-2. *Tellus*, 55B:35–53.
- Ervens, B., Cubison, M., Andrews, E., Feingold, G., Orgen, J. A., Jimenez, J. L., et al. (2007). Prediction of Cloud Condensation Nucleus Number Concentration Using Measurements of Aerosol Size Distributions and Composition and Light Scattering Enhancement Due to Humidity. *J. Geophys. Res.*, 112:D10S32. DOI: 10.1029/2006JD007426.
- Frank, G. P., Dusek, U., and Andreae, M. O. (2006). Technical Note: A Method for Measuring Size-resolved CCN in the Atmosphere. *Atmos. Chem. Phys. Discuss.*, 6:4879–4895.
- Gupta, U. (2008). Valuation of Urban Air Pollution: A Case Study of Kanpur City in India. *Environ. Resource Econ.*, 41:315–326. DOI: 10.1007/s10640-008-9193-0.
- Gupta, T., Chakraborty, A., and Ujwal, K. K. (2010). Development and Performance Evaluation of an Indigenously Developed Air Sampler Designed to Collect Submicron Aerosols. *Annals of the Indian National Academy of Engineering (INAE)*, 7:189–193.
- Houghton, J., Ding, Y., Griggs, D., Noguer, M., van der Linden, P., Dai, X., et al. (2001). *The Science of Climate Change*. Cambridge University Press, Cambridge, UK.
- Hudson, J. G., Xie, Y., and Yum, S. S. (1998). Vertical Distributions of Cloud Condensation Nuclei Spectra Over the Summertime Southern Ocean. *J. Geophys. Res.*, 103:16,609–16,624.
- Hudson, J. G., and Xie, Y. (1999). Vertical Distributions of Cloud Condensation Nuclei Spectra Over the Summertime Northeast Pacific and Atlantic Ocean. *J. Geophys. Res.*, 104:30,219–30,229.

- Hudson, J. G., and Yum, S. S. (2002). Cloud Condensation Nuclei Spectra and Polluted and Clean Clouds Over the Indian Ocean. *J. Geophys. Res.*, 107(D19):8022. DOI: 10.1029/2001JD000829.
- Hudson, J. G., and Frisbie, P. R. (1991). Surface Cloud Condensation Nuclei and Condensation Nuclei Measurements at Reno, Nevada. *Atmos. Environ.*, 25A(10):2285–2299.
- Jurányi, Z., Gysel, M., Weingartner, E., DeCarlo, P. F., Kammermann, L., and Baltensperger, U. (2010). Measured and Modelled Cloud Condensation Nuclei Concentration at the High Alpine Site Jungfraujoch. *Atmos. Chem. Phys. Discuss.*, 10:8859–8897.
- Köhler, H. (1936). The Nucleation in and the Growth of Hygroscopic Droplets. *Trans. Faraday Soc.*, 32:1152–1161.
- Kuwata, M., Kondo, Y., Miyazaki, Y., Komazaki, Y., Kim, J. H., Yum, S. S., et al. (2007). Cloud Condensation Nuclei Activity at Jeju Island, Korea in Spring 2005. *Atmos. Chem. Phys. Discuss.*, 7:15,805–15,851.
- Lance, S., Medina, J., Smith, J. N., and Nenes, A. (2006). Mapping the Operation of the DMT Continuous Flow CCN Counter. *Atmos. Sci. Technol.*, 40:242–254. DOI:10.1080/02786820500543290.
- Lance, S., Nenes, A., Mazzoleni, C., Dubey, M. K., Gates, H., Varutbangkul, V., et al. (2009). Cloud Condensation Nuclei Activity, Closure, and Droplet Growth Kinetics of Houston Aerosol During the Gulf of Mexico Atmospheric Composition and Climate Study (GoMACCS). *J. Geophys. Res.*, 114:D00F15. DOI: 10.1029/2008JD011699.
- Latham, T. L., and Nenes, A. (2011). Water Vapour Depletion in the DMT Continuous Flow CCN Chamber: Effect on Supersaturation and Droplet Growth. *Aeros. Sci. Tech.*, 45(5):604–615. DOI: 10.1080/02786826.2010.551146
- Lixin, S., and Ying, D. (2007). Observations of Cloud Condensation Nuclei in North China. *Acta Meteor. Sinica*, 22:96–106.
- Lohmann, U., and Feichter, J. (2005). Global Indirect Aerosol Effects: A Review. *Atmos. Chem. Phys.*, 5:715–737.
- Mandaria A. K. (2010). *Identification of Air Pollution Sources at Kanpur During Winter Season*. M. Tech thesis, I.I.T. Kanpur.
- Medina, J., Nenes, A., Sotiropoulou, R. P., Cottrell, L. D., Ziemba, L. D., Beckman, P. J., et al. (2007). Cloud Condensation Nuclei Closure During the International Consortium for Atmospheric Research on Transport and Transformation 2004 Campaign: Effects of Size-resolved Composition. *J. Geophys. Res.*, 112:D10S31. DOI: 10.1029/2006JD007588.
- Mehta, B., Venkataraman, C., Bhushan, M., and Tripathi, S. N. (2008). Source Identification at Kanpur During the ISRO-GBP LC-II: Factors Affecting fog Formation. *Atmos. Environ.*, 43:1288–1295.
- Ramanathan, V., Crutzen, P. J., Lelieveld, J., Mitra, A. P., Althausen, D., Anderson, J., et al. (2001). Indian Ocean Experiment: An Integrated Analysis of the Climate Forcing and Effects of the Great Indo-Asian Haze. *J. Geophys. Res.*, 106(D22):28,371–28,398.
- Ramanathan, V., Crutzen, P. J., Kiehl, J. T., and Rosenfeld, D. (2001). Aerosols, Climate and Hydrological Cycle. *Science*, 294:2119–2124.
- Rissman, T. A., VanReken, T. M., Wang, J., Gasparini, R., Collins, D. R., Jonsson, H. H., et al. (2006). Characterization of Ambient Aerosol from Measurements of Cloud Condensation Nuclei During the 2003 Atmospheric Radiation Measurement Aerosol Intensive Observational Period at the Southern Great plains Site in Oklahoma. *J. Geophys. Res.*, 111:D05S11. DOI: 10.1029/2004JD005695.
- Robert, G. C., and Nenes, A. (2005). A Continuous Flow Streamwise Thermal-gradient CCN Chamber for Atmospheric Measurements. *Aeros. Sci. Tech.*, 39:206–221. DOI: 10.1080/027868290913988.
- Rojas, S., Gomes, L., and Villani, P. (2006). Behavior of CCN to CN Fraction During Aging and Mixing Processes of Atmospheric Particles. *Atmos. Chem. Phys. Discuss.*, 6:9545–9562.
- Rose, D., Gunthe, S. S., Mikhailov, E., Frank, G. P., Dusek, U., Andreae, M. O., et al. (2008). Calibration and Measurement Uncertainties of a Continuous-flowcloud Condensation Nuclei Counter (DMT-CCNC): CCN Activation of Ammonium Sulfate and Sodium Chloride Aerosol Particles in Theory and Experiment. *Atmos. Chem. Phys.*, 8:1153–1179.
- Rosenfeld, D., Lohmann, U., Raga, G. B., O'Dowd, C. D., Kumala, M., Fuzzi, S., et al. (2008). Flood or Drought: How do Aerosols Affect Precipitation? *Science*, 321:1309. DOI: 10.1126/science.1160606.
- Roy, A., Baxla, S., Gupta, T., Bandyopadhyaya, R., and Tripathi, S. N. (2009). Measurement of Size Distribution and Chemical Analysis of Particulates Emitted from Indoor Combustion Sources. *Inhal. Toxicol.*, 21:837–848.
- Seinfeld, H. J., and Pandis, N. S. (1998). *Atmospheric Chemistry and Physics, from Air Pollution to Climate Change*. John Wiley, New York.
- Singh, R. P., Dey, S., Tripathi, S. N., and Tare, V. (2004). Variability of Aerosol Parameters Over Kanpur, Northern India. *J. Geophys. Res.*, 109:D23206. DOI: 10.1029/2004JD004966.
- Snider, J., Guibert, S., Brenguier, J., and Putaud, J. (2003). Aerosol Activation in Marine Stratocumulus Clouds: 2. Köhler and Parcel Theory Closures Studies. *J. Geophys. Res.*, 108(D15):8629. DOI: 10.1029/2002JD002692.
- Tare, V., Tripathy, S. N., Chinnam, N., Srivastava, A. K., Dey, S., Manar, M., Kanawade, V., Agarwal, A., Kishore, B., Lal, R. B., and Sharma, M. (2006). Measurement of Atmospheric Parameters During ISRO-GBP Land Campaign II at a Typical Location in Ganga Basin Part-II-chemical Properties. *J. Geophys. Res.*, 111:D23210. DOI: 10.1029/2006JD007279.
- Tripathi, S. N., Dey, S., Tare, V., and Satheesh, S. K. (2005). Aerosol Black Carbon Radiative Forcing at an Industrial City in Northern India. *Geophys. Res. Lett.*, 32:L08802. DOI: 10.1029/2005GL022515.
- Tripathi, S. N., Tare, V., Chinnam, N., Srivastava, A. K., Dey, S., Agarwal, A., et al. (2006). Measurement of Atmospheric Parameters During ISRO-GBP Land Campaign II at a Typical Location in Ganga Basin: Part-I-physical and Optical Properties. *J. Geophys. Res.*, 111:D23209. DOI: 10.1029/2006JD007278.
- VanReken, T. M., Rissman, T. A., Roberts, G. C., Varutbangkul, V., Jonsson, H. H., Flagan, R. C., et al. (2003). Toward Aerosol/Cloud Condensation Nuclei (CCN) Closure During CRYSTAL-FACE. *J. Geophys. Res.*, 108(D20):4633. DOI: 10.1029/2003JD003582.
- Venzac, H., Sellegri, K., Villani, P., Picard, D., and Laj, P. (2008). Seasonal Variation of Aerosol Size Distribution at Puy de Dôme. *Atmos. Chem. Phys. Discuss.*, 8:15,791–15,824.
- Yum, S. S., and Hudson, J. G. (2001). Vertical Distributions of Cloud Condensation Nuclei Spectra Over the Springtime Arctic Ocean. *J. Geophys. Res.*, 106(D14):15,045–15,052.
- Yum, S. S., and Hudson, J. G. (2004). Wintertime/Summertime Contrasts of Cloud Condensation Nuclei and Cloud Microphysics Over the Southern Ocean. *J. Geophys. Res.*, 109:D06204. DOI: 10.1029/2003JD003864.
- Yum, S. S., and Hudson, J. G. (2005). Springtime Cloud Condensation Nuclei Concentrations on the West Coast of Korea. *J. Geophys. Res.*, 32:L09814. DOI: 10.1029/2005GL022641.